Catalysis Today 138 (2008) 28–32

Contents lists available at ScienceDirect

Catalysis Today

journal homepage: www.elsevier.com/locate/cattod

Influence of composition of $MgAl_2O_4$ supported $NiCeO_2ZrO_2$ catalysts on coke formation and catalyst stability for dry reforming of methane

Steven Corthals, Joris Van Nederkassel, Jan Geboers, Hendrik De Winne, Jasper Van Noyen,
Bart Moens, Bert Sels *, Pierre Jacobs *

K.U. Leuven, Centre for Surface Chemistry and Catalysis, Kasteelpark Arenberg 23, 3001 Heverlee, Belgium

ARTICLE INFO

Article history:
Available online 13 June 2008

Keywords:
Dry reforming
Carbon deposition
Spinel
$NiCeO_2ZrO_2/MgAl_2O_4$

ABSTRACT

Dry reforming of methane was studied over Ni catalysts supported on γAl_2O_3, CeO_2, ZrO_2 and $MgAl_2O_4$ (670 °C, 1.5 bar, 16–20 l CH_4 $ml_{catalyst}^{-1}$ h^{-1}). It is shown that $MgAl_2O_4$ supported Ni catalysts promoted with both CeO_2 and ZrO_2 are promising catalysts for dry reforming of methane with carbon dioxide. Within a certain composition range, the simultaneous promotion with CeO_2 and ZrO_2 has great influence on the amount of coke and the catalyst service time. XRD analyses indicate that formation of crystalline $Ce_xZr_{1-x}O_2$ mixed oxide phases occurs on double promotion. In particular, incorporation of low amounts of Zr in the CeO_2 fluorite structure provides stable dry reforming catalysis. As shown with TPR, promotion leads to a higher reduced state of Ni. SEM, XRD and TPR analyses demonstrate that highly dispersed, doubly promoted Ni catalysts with a strong metal-support interaction are essential for stable dry reforming and suppression of the formation of carbon filaments.

1. Introduction

During the last decades, great attention has been paid to dry reforming of CH_4 with CO_2 (1) from the perspective of global warming and alternative energy sources [1,2]. The dry reforming process offers several opportunities. Depending on the kind of energy source used to overcome the reaction endothermicity, dry reforming can be environmental beneficial, since it converts two abundant greenhouse gases into synthesis gas. The produced synthesis gas has a H_2/CO molar ratio typically lower than that of steam reforming, making dry reforming more compatible with Fischer-Tropsch processes for liquid fuel synthesis. Reactions of interest using dry reforming are the conversion of CH_4 (en)rich(ed) in CO_2 and biogas valorisation. Biogas, a mixture of CH_4 and CO_2 produced from the fermentation of biomass and agricultural and industrial food wastes, is a promising renewable energy source [3]. Due to the high CO_2 content, dry reforming could be one of the most suitable processes to convert biogas into synthesis gas. In addition, the transformation of natural gas into synthesis gas recently has attracted great attention since overall reserves of natural gas exceed those of oil [4].

Considerable research efforts have been directed towards the development of active and selective catalysts for CO_2 reforming of CH_4. Coking and metal sintering are obstacles making the development of an industrially applicable catalyst a challenge [5]. The Boudouard reaction (2) and the CH_4 disproportionation (3) are responsible for coke accumulation on the catalyst surface during reaction, leading to deactivation or destruction of the catalysts and a plugged catalyst bed. The high temperature window, necessary for dry reforming, and the formation of H_2O by the reversed water gas shift reaction (4) make the catalyst sensitive to metal sintering. As the critical size of the metal ensembles for catalyzing CH_4 reforming is smaller than that for carbon formation [6], sintering may cause increased amounts of carbon deposits.

$$CH_4 + CO_2 \leftrightarrow 2CO + 2H_2, \qquad \Delta H_{298} = 247\,\text{kJ/mol} \tag{1}$$

$$2CO \leftrightarrow CO_2 + C, \qquad \Delta H_{298} = -172\,\text{kJ/mol} \tag{2}$$

$$CH_4 \leftrightarrow 2H_2 + C, \qquad \Delta H_{298} = 75\,\text{kJ/mol} \tag{3}$$

$$CO_2 + H_2 \leftrightarrow H_2O + CO, \qquad \Delta H_{298} = 41\,\text{kJ/mol} \tag{4}$$

To date, promising catalytic performance has been demonstrated for numerous supported catalysts. In particular, nickel- and noble metal based catalysts [7] show high activity for converting CH_4 with CO_2. Thermodynamic conversions are obtained with

---

* Corresponding authors. Fax: +32 16 32 1998.
E-mail addresses: bert.sels@biw.kuleuven.be (B. Sels), pierre.jacobs@biw.kuleuven.be (P. Jacobs).

0920-5861/$ – see front matter © 2008 Elsevier B.V. All rights reserved.
doi:10.1016/j.cattod.2008.04.038

these catalysts at low contact times but relatively mild process conditions. Although noble metal catalysts are reported to be less sensitive to coking, research on Ni based catalysts is more relevant due to the high cost and low availability of noble metals. Addition of promoters to the Ni catalyst has been shown to prevent at least partially the formation of coke. Bearing in mind the industrial application, it is of utmost importance to use robust supports resistant to temperatures of at least 700 °C.

In this work, we propose a new Ni catalyst formulation comprising both CeO_2 and ZrO_2, supported on $MgAl_2O_4$. $MgAl_2O_4$ has been suggested as a dry reforming support in order to reduce coke formation [8]. Moreover, due to its low acidity and resistance to sintering, $MgAl_2O_4$ has been studied as a stable support in catalytic steam reforming of CH_4 [9]. CeO_2 is an effective promoter for Ni catalysts in dry reforming [10]. Due to its oxygen exchange capacity, CeO_2 reversibly releases and restores a large amount of oxygen atoms. These oxygen species react with surface hydrocarbon species, formed upon CH_4 disproportionation, resulting in reduced formation of coke. As promoter, ZrO_2 is known to enhance CO_2 adsorption on the catalytic surface, also ultimately resulting in reduced formation of coke according to the reversed Boudouard reaction (−2) [11]. Despite the proven beneficial effect of their individual promotion on reforming catalysis, combinations of CeO_2 and ZrO_2, used as promoters, have not been explored extensively [12]. In most cases, mixed oxides of CeO_2 and ZrO_2 are used as a supporting material [13]. It is known that the addition of Zr to CeO_2 improves thermal resistance, redox property and oxygen storage capacity of CeO_2 [14]. DFT calculations suggest an oxygen enhancement by ZrO_2 for CeO_2 catalysts [15]. Due to the insertion of Zr into the CeO_2 framework, the O^{2-} sublattices are distorted, resulting in a higher mobility of oxygen [16]. However, the commercialization of these mixed oxides is difficult due to their high price [12]. Therefore, doubly promoted $Ni/MgAl_2O_4$ catalysts are demonstrated in this work. It is shown that, within a specific composition range of Ni, double promotion with both CeO_2 and ZrO_2 can be beneficial in terms of coke reduction and improved catalyst lifetime under industrially relevant conditions.

2. Experimental

2.1. Catalyst preparation

γAl_2O_3, ZrO_2, CeO_2 and $MgAl_2O_4$ supported catalysts were prepared by incipient wetness impregnation using the support and aqueous solutions of the corresponding metal nitrate salts. The catalysts were dried overnight at 70 °C and calcined at 800 °C for 5 h. γAl_2O_3 (Chem Lab), ZrO_2 (Fluka), CeO_2 (Aldrich) were commercially available supports. The $MgAl_2O_4$ support was prepared as follows. The pH of an aqueous mixture of $Mg(NO_3)_2\cdot 6H_2O$ (Chem Lab) and $Al(NO_3)_3\cdot 9H_2O$ (Riedel-de Haën) was adjusted to 9.5 with an aqueous ammonia solution (Riedel-de Haën). The solution was stirred for 1 h and then ripened overnight. The precipitate was washed with water and dried for 15 h at 120 °C. The resultant powder was then calcined at 800 °C for 5 h. The surface area, measured with N_2 physisorption at liquid N_2 temperature, was $120\ m^2\ g^{-1}$.

2.2. Catalytic tests and characterization

All catalytic tests were carried out in a gas phase continuous flow reactor at 1.5 bar and 670 °C. The reactor furnace contained four parallel fixed bed reactors with internal temperature measurement. The unit is further denoted as quadri-reactor. The quadri-reactor consists out of four tubular quartz tubes (l = 390 mm, i.d. = 3 mm). The catalyst, in 0.125–0.250 mm pellets, was packed on top of a bed of 0.2 g SiC. The solids were retained between two layers of quartz wool. The flow was upstream so that inlet gases were preheated over the SiC bed before passing over the catalyst bed. A mixture of CO_2 and CH_4 was passed over each catalyst tube, the standard molar ratio of the gases being equal to 1.1. The volume hourly space velocity (VHSV) was $16\ l\ CH_4\ ml_{catalyst}^{-1}\ h^{-1}$. Blank samples were taken before reaction when passing the reaction feed over each reactor tube at room temperature. The catalysts were first reduced for 1 h at reaction temperature with an undiluted H_2 stream. Feed and products were analyzed with a digital compact GC of Interscience equipped with a back-flush system. Every 370 s, sampling of another catalyst in the quadri-reactor could be made after on-line analysis. The standard reaction time was 100 min. Thermogravimetric analyses (TGA) of spent catalysts were carried out under an oxidative atmosphere ($O_2/N_2 = 9$) with a TGA Q500 from TA Instruments. The analyzer has a high-throughput sampling platform designed for 16 samples. To discriminate active low-coking catalysts from active high-coking ones, the amount of coke is expressed in mmol C per mole CH_4 converted. SEM investigations of the spent catalysts were performed with a Phillips XL30 FEG microscope. The crystal structure of the catalysts was determined by X-ray powder diffraction. XRD measurements were performed at room temperature with a STOE transmission powder diffractometer system Stadi P Combi equipped with a Cu Kα radiation ($\nu = 1.54$ Å), a Kα1 Germanium Johann-type monochromator and a special designed X/Y high-throughput sampling platform. H_2-TPR experiments were carried out using an Omnistar^{TM} gas analysis system (Pfeiffer vacuum). The catalysts (150 mg) were pretreated in nitrogen at 300 °C for 0.5 h. After cooling to room temperature, H_2/N_2 (5%, $12\ ml\ min^{-1}$) was introduced in the system and the temperature was ramped to 960 °C at a heating rate of $10\ °C\ min^{-1}$. The remaining H_2 was analyzed online.

3. Results and discussion

Most literature reports on dry reforming were performed at high temperature and with diluted gas flows avoiding the coking issue and thus, without direct relevance for industrially significant conditions. Therefore, in this study dry reforming was performed at moderate flow rates without reagent dilution. In addition, reactions at low temperature prevent sintering of Ni, leaving coke formation as the dominant catalyst deactivation process.

Table 1 shows the results obtained for the dry reforming of CH_4 with CO_2 to synthesis gas for γAl_2O_3, ZrO_2, CeO_2 and $MgAl_2O_4$ supported Ni catalysts. The activity of the different only Ni-on-support catalysts (entries 1–4) decreases in the following order: $\gamma Al_2O_3 > MgAl_2O_4 > ZrO_2 > CeO_2$. Irrespective of the slightly lower activity of the $MgAl_2O_4$ supported Ni catalyst compared to γAl_2O_3 (entries 1, 4), the $Ni/MgAl_2O_4$ catalyst forms significantly less coke, in agreement with literature [8]. Due to the higher basicity of the $MgAl_2O_4$ support, more 'acid' CO_2 molecules adsorb on the catalyst surface. The increased surface coverage with CO_2 leads to less carbon deposition as a result of the reversed Boudouard reaction (−2).

Having chosen $MgAl_2O_4$ as the support of choice, we systematically investigated the influence of the Ni, CeO_2 and ZrO_2 content. An increase in the amount of Ni results in higher conversions of CH_4 (X_{CH_4}) and CO_2 (X_{CO_2}) and higher syngas ratios (H_2/CO) (entries 4 and 11). However, higher Ni loadings also lead to more carbon deposition. As stated above, this can be explained by the larger Ni particle size formed with increasing Ni loadings. As promoter, ZrO_2 (entries 5, 12 and 13) and CeO_2 (entries 6, 14 and 15) show a similar effect. Their presence clearly improves the activity of $MgAl_2O_4$ supported Ni catalysts. In case of low Ni loadings, the two promoters also have a beneficial effect on the coke formation

Table 1
Carbon dioxide reforming of methane[a] with Ni(x)CeO$_2$(x)ZrO$_2$(x)-on-support catalysts[b]

Entry	Catalyst	X_{CH_4} (%)	X_{CO_2} (%)	H$_2$/CO	mmol C/mol CH$_{4\ conv}$
1	Ni(10)/γAl$_2$O$_3$	72	80	0.83	19.6
2	Ni(10)/ZrO$_2$	44	56	0.7	0.7
3	Ni(10)/CeO$_2$	32	41	0.49	<0.1
4	Ni(10)/MgAl$_2$O$_4$	67	76	0.82	3.0
5	Ni(10)ZrO$_2$(5)/MgAl$_2$O$_4$	79	87	0.90	7.0
6	Ni(10)CeO$_2$(5)/MgAl$_2$O$_4$	80	87	0.91	37.2
7	Ni(10)CeO$_2$(5)ZrO$_2$(3.3)/MgAl$_2$O$_4$	77	85	0.89	8.6
8	Ni(10)CeO$_2$(5)ZrO$_2$(5)/MgAl$_2$O$_4$	64	66	0.75	2.7
9	Ni(10)CeO$_2$(2.5)ZrO$_2$(2.5)/MgAl$_2$O$_4$	79	87	0.90	14.2
10	Ni(10)CeO$_2$(3.3)ZrO$_2$(5)/MgAl$_2$O$_4$	76	85	0.90	2.0
11	Ni(2)/MgAl$_2$O$_4$	44	58	0.62	0.9
12	Ni(2)ZrO$_2$(3.3)/MgAl$_2$O$_4$	67	74	0.55	0.6
13	Ni(2)ZrO$_2$(5)/MgAl$_2$O$_4$	63	65	0.70	0.8
14	Ni(2)CeO$_2$(3)/MgAl$_2$O$_4$	62	77	0.80	0.7
15	Ni(2)CeO$_2$(5)/MgAl$_2$O$_4$	62	61	0.67	1.0
16	Ni(2)CeO$_2$(2.5)ZrO$_2$(2.5)/MgAl$_2$O$_4$	50	64	0.66	0.6
17	Ni(2)CeO$_2$(5)ZrO$_2$(5)/MgAl$_2$O$_4$	60	73	0.77	0.7
18	Ni(2)CeO$_2$(1.7)ZrO$_2$(5)/MgAl$_2$O$_4$	62	74	0.74	0.5
19	Ni(2)CeO$_2$(4)ZrO$_2$(4)/MgAl$_2$O$_4$	60	75	0.73	0.4
20	Ni(2)CeO$_2$(4.8)ZrO$_2$(0.6)/MgAl$_2$O$_4$	68	76	0.73	0.7

[a] CO$_2$/CH$_4$ = 1.1, T = 670 °C, P = 1.5 bar, VHSV = 16 l CH$_4$ ml$_{catalyst}^{-1}$ h^{-1}.
[b] x in wt%.

(entries 12, 13 and 14) and on the catalytic stability, as shown in Table 1 and Fig. 1. This figure depicts the time dependency of the CH$_4$ conversion for undiluted CH$_4$/CO$_2$ feed at relatively low temperature of 670 °C. As compared to the unpromoted catalyst (entry 11), it is shown that single promotion with ZrO$_2$ (entry 13) or CeO$_2$ (entry 15) improves the catalytic stability. However, these singly promoted catalysts deactivate rapidly within 10 h in the used reaction conditions. To reveal a synergetic promoter effect between CeO$_2$ and ZrO$_2$ on the catalytic stability, we tested several NiCeO$_2$ZrO$_2$/MgAl$_2$O$_4$ catalyst combinations (entries 7–10, 16–20). Some of the compositions clearly showed lower amounts of coke depositions on the catalytic surface without a significant loss of activity. For example, the doubly promoted catalyst (entry 10) exhibits a higher activity than the unpromoted catalyst (entry 4). The conversion of CH$_4$ is approaching the thermodynamic equilibrium in the conditions applied. Moreover, the carbon deposition on the doubly promoted catalysts is in most cases significantly reduced. The effect of the double promotion on the catalytic stability is more clearly presented in Fig. 1 (entries 8 and 20). For catalysts with a low Ni loading, double promotion establishes stable catalytic activity. Indeed, unlike the unpromoted (entry 11) and singly promoted catalysts (entries 13 and 15), the doubly promoted catalyst (entry 20) shows, apart from a small decline in the initial phase, a stable activity without significant deactivation for at least 1600 min on stream in undiluted reagent conditions. Therefore, these low Ni loaded doubly promoted catalysts are a promising candidate for dry reforming of CH$_4$ with CO$_2$. Unlike the low Ni promoted catalysts (entries 11, 13, 15 and 20), the high Ni promoted catalyst (entry 8) plugged in an early stage, as shown in Fig. 1.

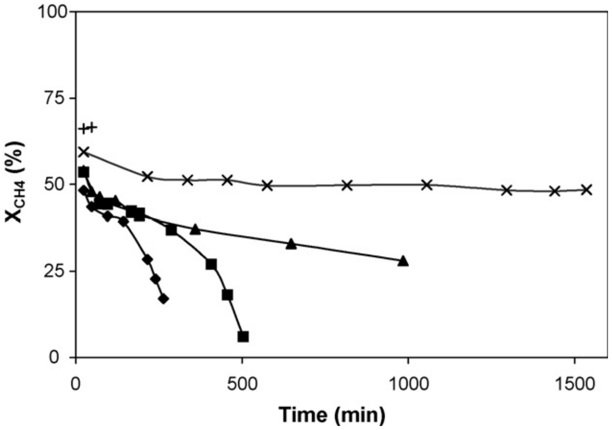

Fig. 1. Time-on-stream behavior of Ni-on-support catalysts for CO$_2$ reforming of CH$_4$. Ni(2)/MgAl$_2$O$_4$ (enty 11, ◆), Ni(2)ZrO$_2$(5)/MgAl$_2$O$_4$ (entry 13, ▲), Ni(2)CeO$_2$(5)/MgAl$_2$O$_4$ (entry 15, ■), Ni(2)CeO$_2$(4.8)ZrO$_2$(0.6)/MgAl$_2$O$_4$ (entry 20, ×) and Ni(10)CeO$_2$(5)ZrO$_2$(5)/MgAl$_2$O$_4$ (entry 8, +); CO$_2$/CH$_4$ = 1.1, T = 670 °C, VHSV = 20 l CH$_4$ ml$_{catalyst}^{-1}$ h^{-1}.

Fig. 2 shows SEM pictures of the plugged catalyst (entry 8) and stable catalyst (entry 20). Carbon filament structures can be seen in both cases. The large number of fibers, formed during dry reforming reaction on the plugged catalyst (entry 8), rapidly causes pore blocking. The number of fibers formed on the stable catalyst (entry 20) during reaction is much lower, even after longer time-on-stream at 670 °C (539 min instead of 98 min in this example). XRD diffraction patterns of calcined MgAl$_2$O$_4$ (a) and two used catalysts, the stable low Ni promoted catalyst (b, entry 20) and the plugged high Ni promoted catalyst (c, entry 8), are shown in Fig. 3. In the case of the used catalysts, the peaks corresponding to the (1 1 1), (2 2 0), (3 1 1) and (4 0 0) reflections of the spinel-like phase indicate maintenance of the catalyst structure during reaction. Diffraction patterns of a CeO$_2$ fluorite structure are clearly shown for the stable catalyst (b, Fig. 3). Detailed inspection of the exact position of the reflections shows a small shift towards higher 2θ values (28.7°, 33.4° and 47.9°) in comparison with the characteristic diffraction patterns of a pure CeO$_2$ fluorite structure (28.5°, 33.3° and 47.8°, 34–394) [17]. Similar values are reported for small Zr substituted CeO$_2$ structures such as Ce$_{0.75}$Zr$_{0.25}$O$_2$ (28–271) with values 28.9°, 48.1° and 57.1°. There are no specific zirconia phases visible in the diffractogram b. Therefore, these results show that some Zr is inserted into the CeO$_2$ fluorite structure with the formation of a Ce$_x$Zr$_{1-x}$O$_2$ mixed oxide structure. No reflections typical of Ni° phases could be recognized in the diffractogram b. In case of the plugged catalyst (c, Fig. 3), the presence of a separate CeO$_2$ fluorite phase is less obvious. The unclear broad envelope around 30° may be due to the formation of a mixture of a CeO$_2$ fluorite structure, a t-ZrO$_2$ phase (30.2°) and a family of highly Zr substituted CeO$_2$ mixed oxides (29.1°) [18]. The diffraction pattern of the plugged catalyst (c, Fig. 3) also shows a Ni° phase with diagnostic reflection at 51.9° in agreement with

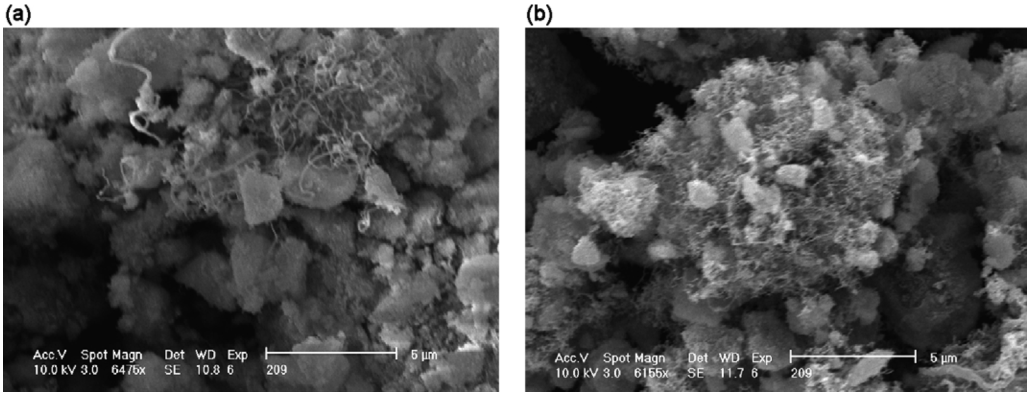

Fig. 2. SEM pictures of Ni(2)CeO_2(4.8)ZrO_2(0.6)/$MgAl_2O_4$ (a, 539 min, entry 20) and Ni(10)CeO_2(5)ZrO_2(5)/$MgAl_2O_4$ (b, 98 min, entry 8) after dry reforming (670 °C, VHSV = 20 l CH_4 $ml_{catalyst}^{-1}$ h^{-1}).

data from Pena et al. [19]. This is consistent with the appearance of a NiO peak (43.2°) in the XRD pattern (not shown) of the freshly prepared catalyst. An additional graphite peak appears at 26.3° in the diffraction pattern of the high Ni promoted catalyst (c, Fig. 3), while even after 539 min at 670 °C, this peak is not detected for the stable catalyst (b, Fig. 3). Combined with the activity tests (see Fig. 1), the XRD analyses demonstrate that a highly dispersed active metal is a necessary condition for stable dry reforming. Low Ni loadings result in small Ni particles. As stated above, stability, coking in particular, depends on the Ni particle size. The results also suggest the formation of mixed oxide phases, such as Zr substituted in CeO_2 crystallites with fluorite structure, is essential for stable dry reforming, because single promotion is not sufficient for stable dry reforming as indicated in Fig. 1.

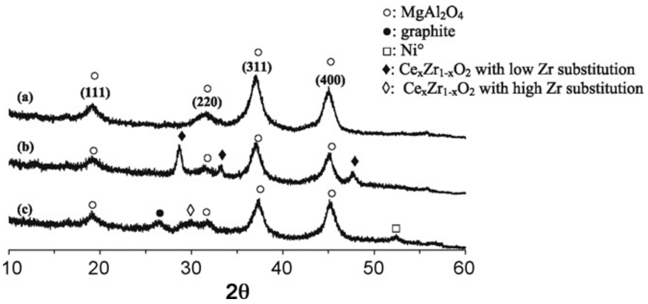

Fig. 3. XRD analyses of $MgAl_2O_4$ (a), Ni(2)CeO_2(4.8)ZrO_2(0.6)/$MgAl_2O_4$ (b, entry 20) and Ni(10)CeO_2(5)ZrO_2(5)/$MgAl_2O_4$ (c, entry 8) (CO_2/CH_4 = 1.1, T = 670 °C, VHSV = 20 l CH_4 $ml_{catalyst}^{-1}$ h^{-1}).

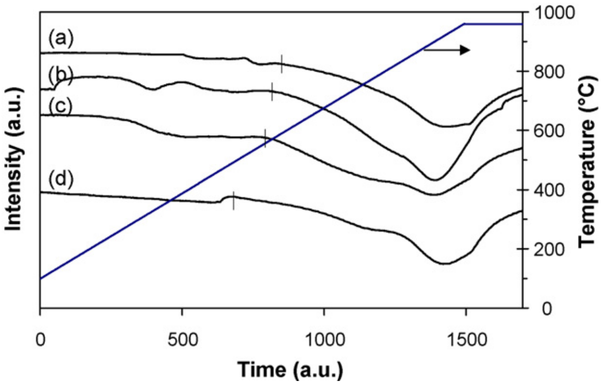

Fig. 4. H_2-TPR experiments of Ni(10)/$MgAl_2O_4$ (a, entry 4), Ni(10)CeO_2(5)/$MgAl_2O_4$ (b, entry 6), Ni(10)ZrO_2(5)/$MgAl_2O_4$ (c, entry 5), Ni(10)CeO_2(5)ZrO_2(5)/$MgAl_2O_4$ (d, entry 8). |: Guide to the eye for the starting point of reduction.

TPR experiments, shown in Fig. 4, were performed to further clarify the role of CeO_2 and ZrO_2. Ni supported on $MgAl_2O_4$ is reduced at a higher temperature as compared to free NiO_x (400 °C), which is an indication for a strong metal-support interaction of Ni with the spinel support. This strong interaction inhibits sintering of Ni particles. Hence, it prevents coking and results in stable dry reforming. The promotion of a Ni loaded catalyst (a, entry 4) with CeO_2 (b, entry 6), ZrO_2 (c, entry 7) or with both (d, entry 8) increases the reducibility of the active element. As shown in Fig. 4, the reduction temperatures of the promoted catalysts shift towards lower values as compared to the unpromoted catalyst (|: guide to the eye for the starting point of reduction). It is well known that CH_4 is activated through donation of σ-electrons of a C–H bond to empty d-orbitals of Ni [20]. Therefore, the increased electron density on Ni lowers carbon deposition via CH_4 disproportionation (3). The augmented reduced state of Ni suppresses the acceptance of σ-electrons, which prevents total decomposition of CH_4 and lowers coking.

SEM, XRD and TPR analyses show that a highly dispersed active Ni with a strong metal-support interaction is necessary for stable dry reforming. Double promotion is essential for stable dry reforming in the used conditions as shown in Fig. 1. The reason for the appearance of this structural and/or chemical promoter effect is not yet totally clear, but XRD analyses suggest the insertion of Zr in fluorite CeO_2 crystallites, when catalysts are promoted with both CeO_2 and ZrO_2. TPR experiments show an increased reducibility of the active element upon promotion. Research will be conducted to further explain these effects and to elucidate the role of the spatial arrangement of the active metal and the promotors.

4. Conclusion

As promoter, CeO_2 and ZrO_2 individually improve the catalytic activity and stability of the Ni/$MgAl_2O_4$ catalysts. For singly promoted catalysts, the improvement of the catalytic stability is still insufficient in the case of undiluted CH_4/CO_2 feed. We here describe a synergistic effect on the catalytic stability of doubly promoted Ni$CeO_2$$ZrO_2$/$MgAl_2O_4$ within a certain composition ranges, allowing stable dry reforming of CH_4 with CO_2 in industrially relevant conditions, in which coke formation was thermodynamically favorable (undiluted reagents at 670 °C). XRD analyses indicate the formation of $Ce_xZr_{1-x}O_2$ mixed oxide phases upon double promotion. For the most stable catalyst Ni(2)CeO_2(4.8)ZrO_2(0.6)/$MgAl_2O_4$, crystalline CeO_2 (fluorite), partially substituted with Zr, was clearly observed, while no separate ZrO_2 phases could be recognized. As shown with TPR, promotion of Ni supported $MgAl_2O_4$ leads to a higher reduced state of Ni, thus reducing the ability of Ni to form coke. Characterization and activity tests demonstrate that highly dispersed, doubly promoted catalysts with a strong metal–support interaction are essential for stable dry reforming. We believe this catalyst combination may serve a new valuable research tool for a better understanding of the relation between coke formation and the surface properties of the catalyst.

Acknowledgements

S.C. acknowledges a Ph.D. grant from the Institute for the Promotion of Innovation through Science and Technology in Flanders (IWT-Vlaanderen). This research is also sponsored by the following research programmes: IAP, GOA and CECAT.

References

[1] M.C.J. Bradford, M.A. Vannice, Catal. Rev.-Sci. Eng. 41 (1999) 1.
[2] A.P.E. York, T.-C. Xiao, M.L.H. Green, J.B. Claridge, Catal. Rev.-Sci. Eng. 49 (2007) 511.
[3] G. Goula, V. Kiousis, L. Nalbandian, I.V. Yentekakis, Solid State Ionics 177 (2006) 2119.
[4] X. Song, Z. Guo, Energy Convers. Manage. 47 (2006) 560.
[5] C.H. Bartholomew, Appl. Catal. A 212 (2001) 17.
[6] J.R. Rostrup-Nielsen, Stud. Surf. Sci. Catal. 68 (1991) 85.
[7] M. Yang, H. Papp, Catal. Today 115 (2006) 199.
[8] J. Guo, H. Lou, H. Zhao, D. Chai, X. Zheng, Appl. Catal. A 273 (2004) 75.
[9] J. Sehested, J. Catal. 217 (2003) 417.
[10] S. Wang, G.Q. Max Lu, Appl. Catal. B 19 (1998) 267.
[11] Y.-Z. Cheng, B.-J. Liaw, W.-H. Lai, Appl. Catal. A 230 (2002) 73.
[12] H.-S. Roh, K.-W. Jun, S.-C. Baek, S.-E. Park, Catal. Lett. 81 (2002) 147.
[13] P. Kumar, Y. Sun, R.O. Idem, Energy Fuels 21 (2007) 3113.
[14] H.-S. Roh, H.S. Potdar, K.-W. Jun, J.-W. Kim, Y.-S. Oh, Appl. Catal. A 276 (2004) 231.
[15] C.T. Campbell, C.H. Peden, Science 309 (2005) 713.
[16] S. Lemaux, A. Bensaddik, A.M.J. Van der Eerden, J.H. Bitter, D.C. Koningsberger, J. Phys. Chem. B 105 (2001) 4810.
[17] S. Damyanova, J.M.C. Bueno, Appl. Catal. A 253 (2003) 135.
[18] J.C. Vargas, S. Libs, A.-C. Roger, A. Kiennemann, Catal. Today 107–108 (2005) 417.
[19] J.A. Pena, J. Herguido, C. Guimon, A. Monzon, J. Santamaria, J. Catal. 159 (1996) 313.
[20] L. Xiancai, W. Min, L. Zhihua, H. Fei, Appl. Catal. A 290 (2005) 81.